ARTICLES

Small-Angle X-ray Scattering Study of Sol−Gel-Derived Siloxane−PEG and Siloxane−PPG Hybrid Materials

Karim Dahmouche,* Celso Valentim Santilli, and Sandra Helena Pulcinelli

Instituto de Química/UNESP, C.P 355, 14800-900 Araraquara-SP, Brazil

Aldo Felix Craievich

Instituto de Física/USP, São Paulo-SP, Brazil

Received: December 4, 1998; In Final Form: March 15, 1999

Hybrid organic−inorganic two-phase nanocomposites of siloxane−poly(ethylene glycol) ($SiO_{3/2}$−PEG) and siloxane−poly(propylene glycol) ($SiO_{3/2}$−PPG) have been obtained by the sol−gel process. In these composites, nanometric siloxane heterogeneities are embedded in a polymeric matrix with covalent bonds in the interfaces. The structure of these materials was investigated in samples with different molecular weights of the polymer using the small-angle X-ray scattering (SAXS) technique. The SAXS spectra exhibit a well-defined peak that was attributed to the existence of a strong spatial correlation of siloxane clusters. $LiClO_4$-doped siloxane−PEG and siloxane−PPG hybrids, which exhibit good ionic conduction properties, have also been studied as a function of the lithium concentration [O]/[Li], O being the oxygens of ether type. SAXS results allowed us to establish a structural model for these materials for different basic compositions and a varying [Li] content. The conclusion is consistent with that deduced from ionic conductivity measurements that exhibit a maximum for [O]/[Li] =15.

1. Introduction

The synthesis of organic−inorganic nanocomposite networks by using the sol−gel process is a rapidly growing research area due to the novel properties and applications of these materials.[1] However, for fine-tunning of a particular property of these materials, a detailed knowledge of their complex molecular structure is required. Generally, the composites can be thought as blends in which the organic and inorganic components form networks that interpenetrate to a certain extent. The properties of the nanocomposites depend on the individual characteristics of the phases and on the nature of the interfaces and are determined by the synthesis pathway employed to manufacture these materials.[2,3]

These composite materials are usually classified according to the type of linking between both networks.[4] In class I materials the organic molecules are simply embedded in the inorganic matrix while in class II materials, the phases are strongly linked by covalent bonds. In both classes, the proximity of the two phases and the exceptionally large interface area result in materials with unusual properties.[5]

Because of the high disorder in molecule arrangement, the small sizes of inorganic or organic clusters and the large differences between the dynamic behavior and chemical interaction in the two phases, the characterization of these materials requires a number of experimental techniques. Small-angle X-ray scattering (SAXS)[6,7] has been used to study structural features of such nanocomposites, while rheology, photon-correlation spectroscopy, NMR relaxation studies,[8,9] fluorescence,[8−10] and forced Rayleigh scattering[11] have been employed to examine the mobility of blend components.

A particularly interesting family of hybrid materials is obtained through the reaction of silicon alkoxides with polyethers.[12,13] Poly(ethylene oxide) or poly(propylene oxide) act as "solid" solvents for many chemical species, while structural inorganic networks are obtained from hydrolysis of reactive silicon species. Hybrids of class I can be obtained by a physical mixture of tetraalkoxysilanes (TMOS or TEOS) with the polymer, leading to the formation of silica−polyether composites (SiO_2−PEO or SiO_2−PPO),[12] while hydrolysis and condensation of trifunctional organosilanes containing covalent attachment of the organic fragment to silicon leads to the obtention of class II siloxane−polyether hybrids ($SiO_{3/2}$−PEO or $SiO_{3/2}$−PPO).[13] Then, materials with a variety of physical properties can be obtained by dissolving suitable doping agents inside such networks. For example, additions of lithium salts and polymetalates, respectively, induce interesting ionic conductivity[13−15] and photochromic properties,[16] while luminescent properties are promoted by rare earth doping.[17]

This is a SAXS study of siloxane−poly(ethylene glycol) ($SiO_{3/2}$−PEG) and siloxane−poly(propylene glycol) (SiO_2−PPG) nanocomposites with covalent bonds between the inorganic (siloxane) and organic (polymer) phases (class II hybrids), in which large quantities of lithium perchlorate can be dissolved. A systematic study has been carried out for several polymer molecular weights and different lithium contents. This work aims at the determination of a structural model to complement previous NMR studies[14,15,18,19] and understand the electrical properties of these materials.

10.1021/jp984605h CCC: $18.00
Published on Web 05/25/1999

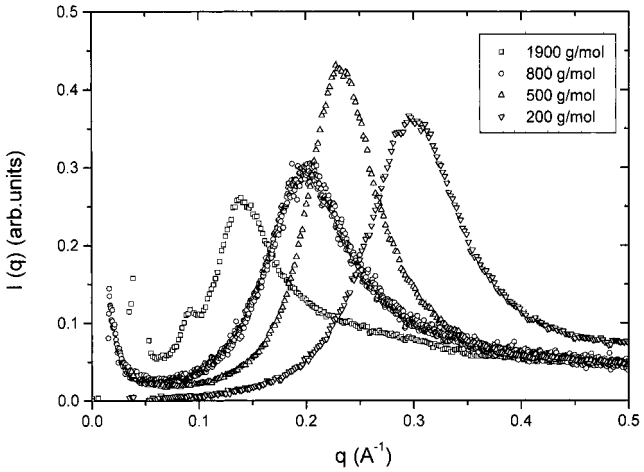

Figure 1. Experimental SAXS intensity $I(q)$ of silica−PEG samples containing polymers of different molecular weights, M_w, prepared using NH_4F as catalyst.

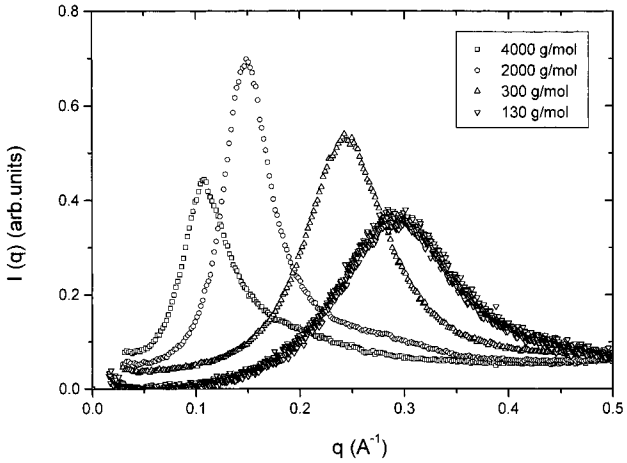

Figure 2. Experimental SAXS intensity $I(q)$ of silica−PPG samples containing polymers of different molecular weights, M_w, prepared using NH_4F as catalyst.

2. Experimental Section

Equimolar amounts of (3-isocyanatopropyl)triethoxysilane (IsoTrEOS) and *O*,*O*′-bis((2-aminopropyl)poly(ethylene glycol)) or *O*,*O*′-bis((2-aminopropyl)poly(propylene glycol)) were stirred together in tetrahydrofuran (THF) under reflux for 6 h. THF was evaporated and a pure hybrid precursor $(OEt)_3Si-(PEG$ or $PPG)-Si(OEt)_3$ was obtained. A 0.5 g sample of this precursor was mixed with 1 mL of ethanol containing NH_4F ($[NH_4F]/[Si] = 0.005$). Finally, water ($[H_2O]/[Si] = 6$) was added upon stirring and a monolithic wet gel was obtained in 4 h. Ethanol was then slowly removed at 50 °C to give a body of rubbery like material. The chemical reagents were purchased from Fluka and Aldrich.

The X-ray scattering study was performed using the SAXS synchrotron beamline of LNLS (Campinas, Brazil). The beamline is equipped with an asymmetrically cut and bent silicon (111) monochromator that yields a monochromatic ($\lambda = 1.68$ Å) and horizontally focused beam. A vertical position-sensitive X-ray detector and a multichannel analyzer were used to record the SAXS intensity, $I(q)$, as a function of the modulus of the scattering vector $q = 4\pi \sin(\epsilon/\lambda)$, ϵ being the scattering angle. Each SAXS spectrum corresponds to a data collection time interval of 300 s. Because of the small size of the incident beam cross section at the detection plane, no mathematical desmearing of the experimental SAXS intensity function was needed.

The SAXS intensity, $I(q)$, is proportional to the Fourier transform of the correlation function of the electronic density of the material. $I(q)$ was determined (in arbitrary units) as the difference between the experimental SAXS intensity recorded with the sample and the parasitic scattering curve obtained under similar conditions without sample. Appropriate normalization was performed to account for sample attenuation and natural decay in intensity of the incident beam. A constant intensity background due to the statistic electronic short-range electron density fluctuations was removed using Porod's plots ($I(q)q^4$ versus q^4), which exhibit a linear regime for all the studied materials.

3. Results and Discussion

3.1. Effect of the Polymer Molecular Weight. Figure 1 shows SAXS spectra corresponding to several siloxane−PEG samples containing polymers of different molecular weight, M_w, prepared using a NH_4F catalyst. Similar spectra are plotted in Figure 2 corresponding to siloxane−PPG samples prepared under equivalent conditions and varying also the polymer molecular weight.

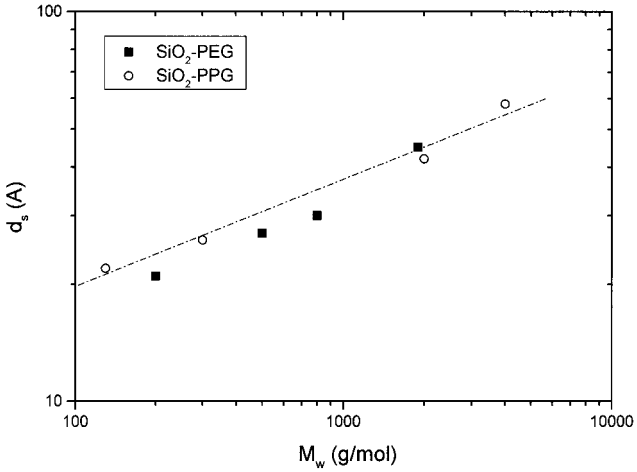

Figure 3. Average particle distance d_s as a function of the polymer weight M_w in log−log scale for silica−PEG and silica−PPG blends.

All spectra exhibit a single peak with a maximum located at different q values for different molecular weights. We assume this peak is an interference effect in X-ray scattering amplitude produced by the existence of a strong spatial correlation between siloxane heterogeneities or clusters embedded in the polymeric matrix. Since there are no reasons for the sizes of the clusters to be all equal, it is expected that the assumed spatial correlation is not strong enough to produce high-order interference peaks in SAXS spectra. Therefore, SAXS curves plotted in Figures 1 and 2 are similar to those corresponding to the wide-angle scattering produced by very disordered atomic structures. Under this assumption, an average and most probable distance between siloxane clusters (d_s) can be estimated by

$$d_s = 2\pi/q_{max} \quad (1)$$

q_{max} being the modulus of the scattering vector at the peak maximum.[20] If the above specified assumption is really true, we would a priori expect to observe an increase in the average distance for increasing polymer molecular weight. Figure 3 shows the average intercluster distance d_s as a function of the polymer molecular weight in log−log scale for siloxane−PEG and siloxane−PPG blends. We note that both series of samples exhibit the expected increase in the distance d_s for increasing M_w.

The results presented in Figure 3 demonstrate that the average distances between siloxane clusters, chemically cross-linked at the end of oligomeric chains, are determined by the length of the polymer chain and not appreciably by its nature. In addition, the fact that $d_s \propto M_w^{1/3}$ indicates that the polymers are in a highly folded and entangled configuration. As a matter of fact, a more or less extended configuration would lead to an exponent value near 1.

We can obtain additional information from the integral of the SAXS function plotted in Figures 1 and 2. For a two-electron density model (in our case the siloxane clusters and polymer matrix) the integral Q is given by[20]

$$Q = \int_0^\infty I(q)q^2\,\mathrm{d}q = 2\pi^2(\rho_s - \rho_p)^2 V\phi_s\phi_p \qquad (2)$$

where V is the irradiated volume, ϕ_s and ρ_s are respectively the volume fraction and electron density of siloxane heterogeneities, and ϕ_p and ρ_p are respectively the volume fraction and electronic density of the polymeric matrix.

For small ϕ_s (i.e., a dilute system), eq 2 becomes

$$Q = 2\pi^2(\rho_s - \rho_p)^2\phi_s V \qquad (3)$$

the product $\phi_s V$ being the partial volume V_p occupied by the "solute" siloxane phase.

Another parameter that contains structural information is the Porod constant, A_p, defined as follows:[20]

$$A_p = \lim_{q\to\infty} I(q)q^4 = 2\pi(\rho_s - \rho_p)^2 S \qquad (4)$$

S being the interface area between the two phases in the irradiated volume. The ratio Q/A_p yields

$$Q/A_p = \pi\phi_s\phi_p/(V/S) \qquad (5)$$

In the simplest case of a "dilute" system of spherical and monodisperse set of particles of radius R_p, eq 5 becomes

$$Q/A_p = \pi R_p/3 \qquad (6)$$

The volume fractions ϕ_s and ϕ_p were determined from the density of the sample measured by helium pycnometry and by assuming that the phases consist of pure siloxane or pure polymer. We used the density values 2.20, 1.12, and 1.01 g/cm^3 for the siloxane clusters, PEG, and PPG, respectively.

The siloxane cluster size was determined by assuming spherical particles of radius R_s forming a compact arrangement. Under these assumptions the following relation holds:[13]

$$R_s = (3\phi_s/8\pi)^{1/3}(d_s/2) \qquad (7)$$

Additional information about the degree of order of the siloxane clusters arrangement can be obtained from the width of the SAXS peak. An average size of the correlation volume associated with the spatial distribution of siloxane clusters (i.e., an estimate of the size of the very disordered "supercrystal"), L_C, can be obtained by applying the Scherrer equation in the case of low-angle X-ray scattering:

$$L_C = 4\pi/\Delta q \qquad (8)$$

where Δq is the full width at half-maximum (fwhm) of the correlation peak of the SAXS function.

The dependence of Q and A_p are plotted in Figure 4 as functions of the molecular weight for siloxane−PEG and siloxane−PPG blends. We can see that both functions exhibit a similar trend: they decrease for increasing molecular weight. A similar behavior is observed for both studied blends. We also plotted in Figure 4 the volume fraction of the siloxane clusters, ϕ_s, calculated, as explained above, from the nominal composition of the blends. Hybrids containing polymers with higher molecular weight and equivalent stoichiometry would produce a two-phase system with a decreasing partial volume fraction of the phase occupied by siloxane clusters and, consequently, with a decreasing interface area. The similar qualitative dependence on M_w of the parameters Q, A_p, and ϕ_s, shown in Figure 4 confirms the mentioned expectation. The good correlation of Q and A_p with the volume fraction of the siloxane clusters implies that the variations of theses parameters are mainly due to the variation of ϕ_s. This means that eventual variations in the electronic phase contrast and effects of the nature of the polymer studied do not play an appreciable role on the structural features of the studied materials.

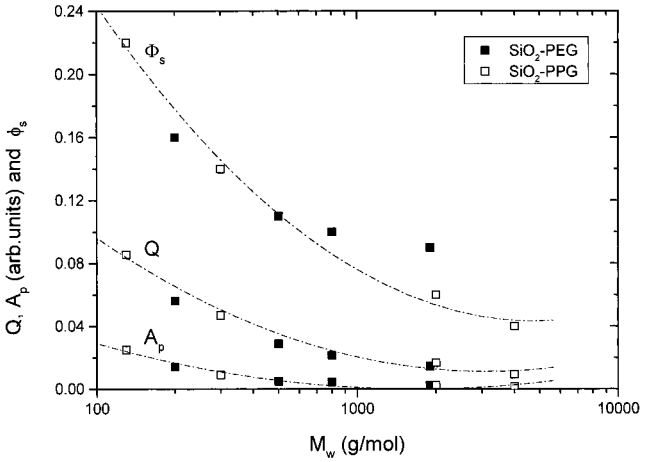

Figure 4. Dependence of the integral $Q = \int_0^\infty I(q)q^2\,\mathrm{d}q$, the Porod constant A_p, and the volume fraction of silica particles ϕ_s as a function of the polymer molecular weight M_w for silica−PEG and silica−PPG blends.

All these results are consistent with the basic structural model of isolated siloxane clusters embedded in a polymeric matrix in both studied blends. The partial volume being occupied by the clusters depends essentially of the volume proportion of siloxane phase and polymer, the density of particles and matrix being independent of the molecular weight.

Another topic investigated is the effect of molecular weight on the size of the siloxane heterogeneities. The radii of the clusters were calculated using two independent equations ((6) and (7)). Equation 6 uses the invariant Q and the Porod's constant A_p, while eq 7 is based on the knowledge of the scattering peak position (leading to d_s). The respective R_p and R_s values obtained as a function of the polymer molecular weight M_w are plotted in Figure 5. The reasonable agreement between R_p and R_s demonstrates the consistence of the two-phase (pure polymer and pure siloxane phase) structural model proposed.

The values obtained by SAXS for all siloxane clusters radii (between 2.8 and 6.5 Å) are coherent with ^{29}Si NMR results obtained in siloxane−PEG samples (PEG molecular weight = 800) prepared in the same conditions.[19] The notation T^1, T^2, T^3, and T^4 is used to represent the number of connections that each silicate makes through oxygen bridges with silicon neighbors. The relative abundance of the T^1, T^2, and T^3 silicon nuclei (calculated from the integrated intensities of the resonances in the ^{29}Si NMR spectra) is respectively 23%, 74%, and 3% and reveals that the material is 45% condensed. This condensation degree is quite lower than that obtained in other

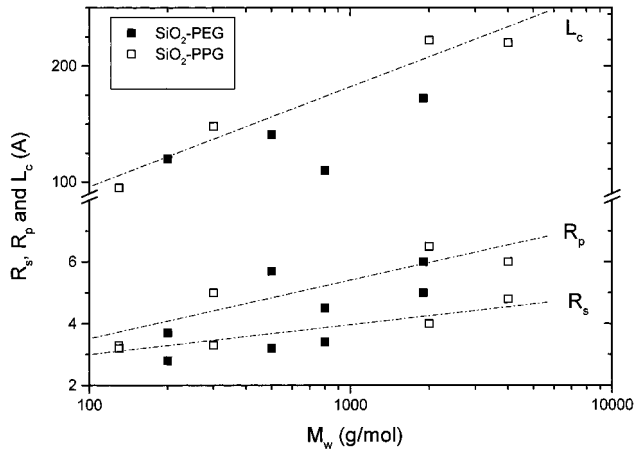

Figure 5. Dependence of the particle radius R_p and R_s (calculated using eqs 6 and 7, respectively) and the average size of the correlation volume L_C as a function of the polymer molecular weight M_w for silica−PEG and silica−PPG blends.

siloxane−polymer hybrid materials such as polysilsesquioxanes [21] or POSS.[22,23] However, it indicates that, as observed in these systems, the siloxane clusters are incompletely condensed and consequently open frameworks of nanometric size.

We note in Figure 5 a clear increase in the size of the siloxane clusters radius for increasing molecular weight. From M_w = 130 up to 4000 there is an aproximate variation of 45%. This is probably due to the conditions of formation of these clusters in the precursor sol. For high M_w, hydroxyl groups Si−OH located at the end of a polymer chain can polycondensate with other groups located at the end of different polymer chains and also with the groups located at the opposite extremity of the same chain. Since the rigidity of polymer chains increases for decreasing chain length,[24] we expect that the polycondensation process of Si−OH groups belonging to the same chain will be less probable in hybrids containing short polymer. Therefore the resulting average radius of siloxane clusters is expected to be smaller in such materials.

Beside a decrease in overall integrated intensity, an increase in the broadening of the interference peak is observed in Figures 1 and 2 for decreasing molecular weight. This implies that the correlation size of the clusters arrangement, L_C, is smaller for shorter molecules, as can be seen in Figure 5. This is expected because a lower intercluster distance d_s implies a smaller size of the correlation domains.

3.2. Effect of the Amount of Catalyst. The observed dependence between the phase separation process and the reactivity of silicon alkoxide toward polycondensation reactions led us to vary the amount of catalyst, the molecular weight of the PEG remaining constant (800). The SAXS results obtained for various amounts of NH_4F are shown in Figure 6.

The SAXS spectra show again the presence of an interference peak, its position, and consequently the average distance between siloxane clusters, remaining practically invariant ($d_s \cong 30 \pm 1$ Å). This suggests that the general morphology of the material does not depend on the amount of catalyst. We plotted in Figure 7 the integral Q as a function of the content of NH_4F. We can see that a decrease in catalyst content produces a strong clear decrease in the integral Q. This is attributed to the incomplete hydrolysis and polycondensation of silicon species. Therefore, the volume fraction of siloxane clusters ϕ_s is reduced and some silicon species are dispersed in the polymer matrix, decreasing the electronic density contrast ($\rho_s - \rho_p$).

This interpretation is confirmed by the decrease of the

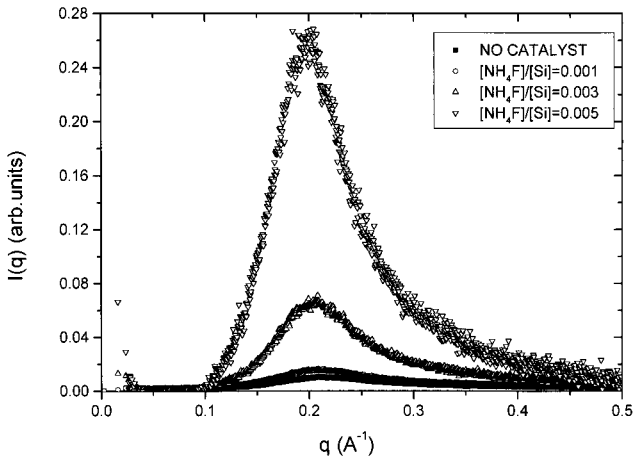

Figure 6. Experimental SAXS intensity $I(q)$ of silica−PEG hybrids (M_w = 800) obtained for different [NH_4F]/[Si] ratios.

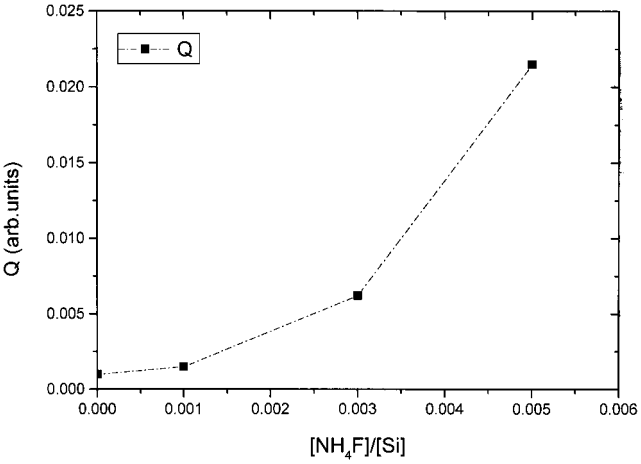

Figure 7. Dependence of the integral $Q = \int_0^\infty I(q)q^2\,dq$ on [NH_4F]/[Si] for silica−PEG hybrids (M_w = 800).

correlation size of the particle arrangement, L_C, from 120 to 108 Å as the ratio [NH_4F]/[Si] decreases from 0.005 to 0.

3.3. Effect of the Lithium Concentration. Li^+ is generally selected as a charge carrier to obtain solid electrolytes based on ionic conductor polymers. We have studied the effect of the content of this cation on the structural features of siloxane−PPG_{2000} samples catalyzed by NH_4F ([NH_4F]/[Si] = 0.005).

The ionic conductivity of siloxane−PEG and siloxane−PPG class II nanocomposites increases for increasing doping level up to [O]/[Li] = 15.[14−16] At higher doping levels, a progressive decrease in conductivity occurs. So a maximum of ionic conductivity is observed in both blends for [O]/[Li] = 15. It is well established that ionic conductivity occurs along the amorphous phase of the polymer, via a liquidlike motion of Li^+ ions through the segmental motions of neighboring chains.[25] For increasing Li content, at high salt concentration ([O]/[Li] < 15), the mechanism responsible for the decrease in conductivity is related to a progressive decrease in ionic mobility. This effect is attributed to the formation of cross-linking O−Li^+−O between oxygen atoms of different polymer chains, which leads to a decrease in their mobility or to cation−anion interactions. These interactions may form polymer (solvent) separated pairs, contact ion pairs, ionic multiplets, or even salt aggregates.

SAXS spectra of samples containing different amounts of lithium [O]/[Li] (the oxygens are those of the ether type) are shown in Figure 8.

For low doped samples ([O]/[Li] ≥ 15) the peak position is essentially invariant, revealing that the average distance between

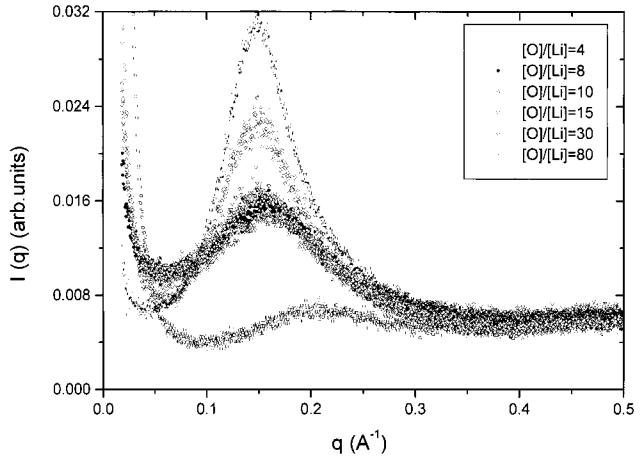

Figure 8. Experimental SAXS intensity $I(q)$ of silica−PPG hybrids ($M_w = 2000$) obtained for different [O]/[Li] ratios and prepared using NH_4F as catalyst.

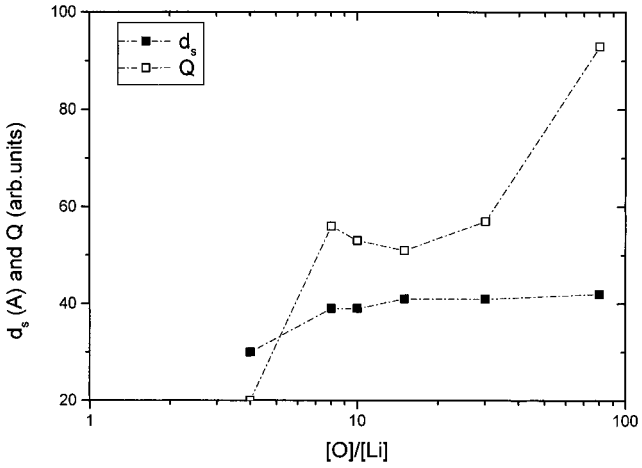

Figure 9. Dependence of the integral $Q = \int_0^\infty I(q)q^2\,dq$ and the average interparticle distance d_s as a function of [O]/[Li] for silica−PPG hybrids ($M_w = 2000$) prepared using NH_4F as catalyst.

the siloxane clusters, d_s, remains invariant for different Li^+ doping. A different behavior is observed for the SAXS integral, Q, which decreases as the doping increases (Figure 9). The average distance between siloxane heterogeneities remaining constant, the decrease in the integral Q was attributed to the decrease in electron density contrast, $\rho_s - \rho_p$ (see eq 2) as a consequence of a progressive filling effect of the increasing amount of Li^+ interacting with the ether type oxygens and occupying the open space between polymeric chains.

For high Li^+ content ($8 \le [O]/[Li] \le 15$), the SAXS peak position shifts toward high q values, indicating a decrease of the average distance between siloxane clusters, d_s, as the doping increases. This behavior suggests that the structure of the polymer becomes more and more contracted as a consequence of the increase in the degree of cross-linking O−Li^+−O between polymeric chains. On the other hand, as the contraction of the polymer occurs, its density should increase and consequently the contrast between the electronic density of the two phases ($\rho_s - \rho_p$) should decrease. At the same time, as the siloxane intercluster spacing d_s decreases, the siloxane volume fraction ϕ_s should increase. These two simultaneous phenomena should lead to small variations of Q (see eq 3). However, the increase of ϕ_s seems to be sligthly predominant because a noticeable increase in Q is observed when the Li^+ concentration is increased from [O]/[Li] = 15 to [O]/[Li] = 8.

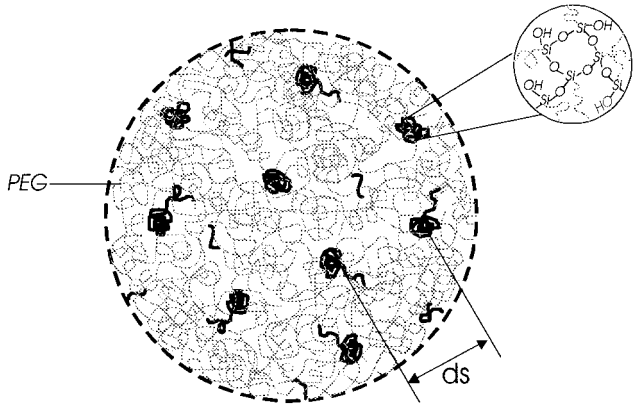

Figure 10. General morphological model for siloxane−PEG nanocomposites. The average distance between the siloxane clusters is indicated by the letter d_s.

For extremely high salt concentration ([O]/[Li] = 4), the peak position shows a strong shift to higher q and the value of d_s is decreased ($d_s = 30$ Å). The large broadness of the peak for high Li^+ content indicates that the spatial correlation size L_C of siloxane clusters arrangement becomes less defined, probably because of a more complex nature of the material. At very high Li^+ content the model of only two electronic density structures does not hold, probably because of an incipient segregation of a lithium rich phase.

4. Conclusions

We investigated the structure of organic−inorganic PEG−siloxane and PPG−siloxane blends presenting covalent bonds between the siloxane phase and the polymer chains (class II hybrids). The structural features deduced from SAXS results indicate the existence of a phase separation process at a nanometric scale.

The composite is a two-phase system composed of dispersed and spatially correlated siloxane nanoclusters, chemically cross-linked at the ends of the polymeric chains and forming a homogeneous matrix (Figure 10). The validity of Porod's law for all the studied samples corroborates the two-phase model proposed for the studied materials.

The increase in siloxane heterogeneities average distance in samples containing polymer molecules with higher molecular weight, deduced from SAXS results, confirms that the peak in the scattering spectra is produced by interference effects associated with the spatial correlation between isolated siloxane clusters. This study also demonstrated that the polymer chains are strongly folded and entangled and form a nearly homogeneous continuous matrix.

The polycondensation of silicon species and the correlation size of the cluster arrangement can be controlled by the amount of catalyst.

The studied nanocomposites exhibit an increasing ionic conductivity for increasing lithium doping level up to [O]/[Li] = 15. For larger amounts of lithium ions added, the formation of cross-linking between oxygen atoms of polymer chains induces a decrease in chain mobility and so in ionic conductivity. For an extremely high doping level ([O]/[Li] = 4) the segregation of a lithium rich phase should occur, leading also to the decrease of ionic conduction properties.

These advanced materials should be of great technological interest for optical applications such as solid-state electrochromic devices or automotive mirrors where a solid, transparent, and flexible ionic conductor is required.

Acknowledgment. The authors acknowledge the collaboration of LNLS staff during SAXS experiments and financial support from FAPESP and PRONEX.

References and Notes

(1) *Proceeding of the First European Workshop on Hybrid Organic−Inorganic Materials*, Bierville, 1993 (Sanchez, C., Ribot, F., Eds.).

(2) Novak, B. M. *Adv. Mater*. **1993**, *5*, 422.

(3) Schmidt, H. *Spectroscopy and Applications of Sol−Gel Glasses*; Springer-Verlag: Berlin, 1992.

(4) Sanchez, C.; Ribot, F. *New J. Chem*. **1994**, *18*, 1007.

(5) Judeinstein, P.; Sanchez, C. *J. Mater. Chem.* **1996**, *6*, 511.

(6) Rodrigues, D. E.; Brennan, A. B.; Betrabet, C.; Wang, B.; Wilkes, G. L. *Chem. Mater*. **1992**, *4*, 1437.

(7) Beaucage, G.; Ulibarri, T. A.; Black, E. P.; Schaefer, D. W. *Hybrid Organic−Inorganic Composites*; ACS Symposium Series No. 585; American Chemical Society: Washington, DC, 1995; p 97.

(8) Winter, R.; Hua, D. W.; Song, X.; Mantulin, W.; Jonas, J. *J. Phys Chem.* **1990**, *94*, 2706.

(9) Judeinstein, P.; Oliveira, P. W.; Bayle, J. P.; Courtieu, J. *J. Chim. Phys.* **1994**, *91*, 1583.

(10) Hanna, S. D.; Dunn, B.; Zink, J. *MRS Symp. Proc*. **1992**, *271*, 651.

(11) Judeinstein, P.; Oliveira, P. W.; Krug, H.; Schmidt, H. *Chem. Phys. Lett*. **1994**, *220*, 35.

(12) Ravaine, D.; Seminel, A.; Charbouillot, Y.; Vincens, M. *J. Non. Cryst. Solids* **1986**, *82*, 210.

(13) Judeinstein, P.; Titman, J.; Stamm, M.; Schmidt, H. *Chem. Mater*. **1994**, *6*, 127.

(14) Dahmouche, K.; Atik, M.; Mello, N. C.; Bonagamba, T. J.; Paneppucci, H.; Aegerter, M. A.; Judeinstein, P. *J. Sol-Gel Sci. Technol*. **1997**, *8*, 711.

(15) Dahmouche, K.; De Souza, P. H.; Bonagamba, T. J.; Paneppucci, H.; Judeinstein, P.; Pulcinelli, S. H.; Santilli, C. V. *J. Sol-Gel Sci. Technol*. **1998**, *13*, 909.

(16) Judeinstein, P.; Schmidt, H. *J. Sol-Gel Sci. Technol*. **1994**, *3*, 189.

(17) Ribeiro, S. J. L.; Dahmouche, K.; Ribeiro, C. A.; Santilli, C. V.; Pulcinelli, S. H. *J. Sol-Gel Sci. Technol*. **1998**, *13*, 427.

(18) Dahmouche, K.; Atik, M.; Mello, N. C.; Bonagamba, T. J.; Paneppucci, H.; Aegerter, M. A.; Judeinstein, P. *MRS. Symp. Proc.* **1996**, *435*, 363.

(19) Mello, N. C. Ph.D. Thesis, Instituto de Física de São Carlos (USP), 1998.

(20) Glatter, O.; Kratky, O. *Small-Angle X-ray Scattering*; Academic Press: New York, 1982.

(21) Loy, D. A.; Shea, K. J. *Chem. Rev*. **1995**, *95*, 1431.

(22) Lichtenhan, J. D.; Noel, C. J.; Bolf, A. G.; Ruth, P. N. *MRS. Symp. Proc.* **1996**, *435*, 3.

(23) Feher, F. J.; Newman, D. A *J. Am. Chem. Soc*. **1990**, *112*, 1931.

(24) Brik, M.; Titman, J.; Bayle, J. P.; Judeinstein, P. *J. Polym. Sci., Polym. Phys.* **1996**, *34*, 2533.

(25) Gray, F. M. *Solid Polymer Electrolytes, Fundamental and Technological Applications*; VCH: New York, 1991.